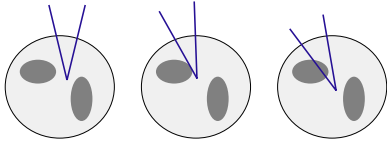


## Electrical impedance tomography and Mittag-Leffler's function



**Samuli Siltanen** ([samuli.siltanen@iki.fi](mailto:samuli.siltanen@iki.fi))  
 Gunma University (JSPS Fellow)  
 Instrumentarium Imaging, Finland

4th Matsuyama Analysis Seminar  
 Ehime University, February 17, 2004

## This is a joint work with

**Masaru Ikehata**

Gunma University, Japan

**David Isaacson**

Rensselaer Polytechnic Institute, USA

**Kim Knudsen**

Aalborg University, Denmark

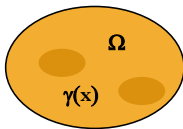
**Jennifer Mueller**

Colorado State University, USA

**Jon Newell**

Rensselaer Polytechnic Institute, USA

## The inverse conductivity problem of Calderón



$$\Lambda_\gamma f = \gamma \frac{\partial u}{\partial \nu} \Big|_{\partial \Omega},$$

$$\begin{aligned} \nabla \cdot \gamma \nabla u &= 0 \text{ in } \Omega, \\ u &= f \text{ on } \partial \Omega. \end{aligned}$$

*Uniqueness:* Is the conductivity  $\gamma$  uniquely determined by the Dirichlet-to-Neumann (DN) map?

*Reconstruction:* If uniqueness holds, how to reconstruct the conductivity from the knowledge of the DN map?

## The inverse conductivity problem is nonlinear

The weak formulation of the DN map as an operator

$$\Lambda_\gamma : H^{1/2}(\partial \Omega) \rightarrow H^{-1/2}(\partial \Omega),$$

is given by

$$\langle \Lambda_\gamma f, g \rangle = \int_{\Omega} \gamma \nabla u \cdot \nabla v,$$

where  $v$  is any  $H^1$  function with trace  $g$ , and  $u$  satisfies the Dirichlet problem

$$\begin{cases} \nabla \cdot \gamma \nabla u = 0 & \text{in } \Omega, \\ u = f & \text{on } \partial \Omega. \end{cases}$$

Clearly, the map  $\gamma \mapsto \Lambda_\gamma$  is nonlinear.

## The inverse conductivity problem is ill-posed in the sense of Hadamard

Large changes in  $\gamma$  correspond to small changes in the DN map.

Thus, the conductivity does not depend continuously on the measurement data.

## The uniqueness question in 2-D has been studied by these authors

**1980** Calderón

**1985** Kohn and Vogelius (piecewise real-analytic  $\gamma$ )

**1987** Sylvester and Uhlmann ( $n > 2$ )

**1987** R G Novikov ( $n > 2$ )

**1988** Nachman ( $n > 2$ )

**1996** Nachman ( $\gamma$  has two weak derivatives)

**1997** Brown and Uhlmann ( $\gamma$  has one weak derivative)

**2003** Astala and Päivärinta ( $\gamma$  essentially bounded)

**EIT reconstruction algorithms can be divided roughly into the following classes:**

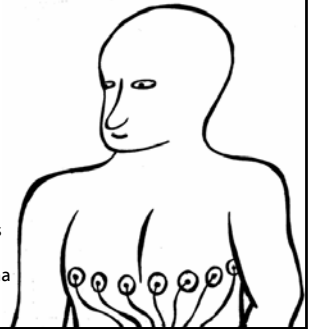
- Linearization
- Iterative output least-squares methods
- Statistical inversion
- The inverse scattering approach, or d-bar method
- Recovery of partial information (discontinuities)

**Electrical impedance tomography (EIT) is an emerging medical imaging method**

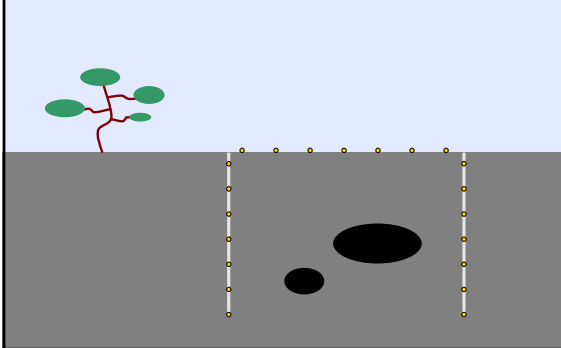
Feed electric currents through electrodes, measure voltages

Reconstruct the image of electric conductivity in a two-dimensional slice

Applications include: monitoring heart and lungs of SARS patients, detecting pulmonary edema (swollen lungs)



**Geological sensing of oil or metals is another application of EIT**



**In this talk we discuss two approaches to the practical reconstruction problem**

We present a d-bar method for reconstructing smooth conductivities that equal to 1 near the boundary

We show how to use Mittag-Leffler's function to recover discontinuities in a homogeneous background conductivity

(We always take  $\Omega$  to be the unit disc in the plane)

**For application of theoretical results to EIT, we must consider some practical issues**

- Currents are applied and voltages measured
- Measurements are done with electrodes
- There is a finite number of measurements
- Measurements contain random errors (noise)

**Current-to-voltage measurements are described with the ND map**

The Neumann-to-Dirichlet (ND) map is defined by

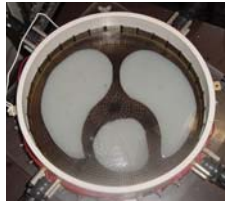
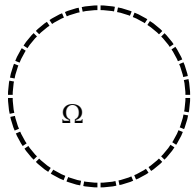
$$R_\gamma f = u|_{\partial\Omega} - \frac{1}{|\partial\Omega|} \int_{\partial\Omega} u,$$

where  $u$  satisfies the Neumann problem

$$\begin{cases} \nabla \cdot \gamma \nabla u = 0 & \text{in } \Omega, \\ \frac{\partial u}{\partial \nu} = f & \text{on } \partial\Omega. \end{cases}$$

In practice, currents are applied and voltages measured. This is because the ND operator is smoothing and suppresses noise, while the DN operator is roughing and amplifies noise.

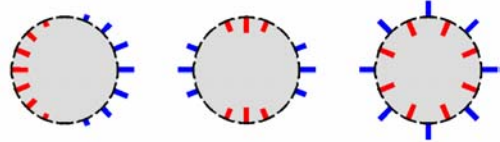
**This is a typical configuration for electrode measurements in EIT**



Here we have N=32 electrodes.  
The machine is in Rensselaer Polytechnic Institute, USA.

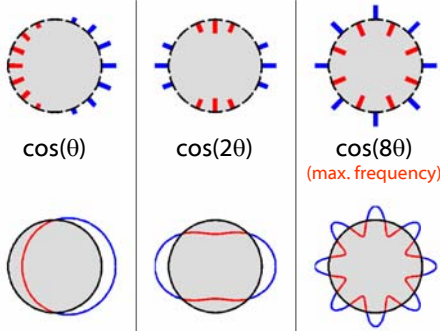
**There is a finite number of linearly independent current patterns**

Here are three examples with N=16:



Altogether, there are N-1 linearly independent current patterns due to conservation of charge.

**We approximate the discrete currents by continuous Neumann data. Here N=16.**



**We simulate a finite set of EIT measurements with a complex 32x32 matrix**

$$\text{Let } \phi_k = (2\pi)^{-1/2}(x_1+ix_2)^k|_{\partial\Omega}, \quad k \in \mathbb{Z}.$$

We solve the Neumann problem

$$\nabla \cdot \gamma \nabla u_k = 0 \text{ in } \Omega, \quad \gamma \frac{\partial u_k}{\partial \nu} = \phi_k \text{ on } \partial\Omega,$$

for  $k = -15, \dots, 16$ . Further, we set

$$\mathcal{R}_\gamma [l, k] = \int_{\partial\Omega} u_k \bar{\phi}_l \, d\sigma,$$

and add Gaussian random numbers to the elements of  $\mathcal{R}_\gamma$  to simulate measurement noise.

**Studies on d-bar reconstruction methods**

Based on Nachman (1996) or Brown and Uhlmann (1997)

- 2000 **Siltanen, Mueller and Isaacson**
- 2002 **Mueller, Siltanen and Isaacson**
- 2003 **Mueller and Siltanen**
- 2003 **Knudsen**
- 2003 **Knudsen and Tamasan**
- to appear **Knudsen, Mueller and Siltanen**
- submitted **Isaacson, Mueller, Newell and Siltanen**

**Nachman's 1996 proof consists of two steps:**

$$\Lambda_\gamma \rightarrow \mathbf{t} \rightarrow \gamma$$

The intermediate object  $\mathbf{t}$  is a complex-valued function called *scattering transform* and defined as follows for complex  $k$ :

$$\mathbf{t}(k) := \int_{\mathbb{R}^2} e^{i\bar{k}\bar{x}} q(x) \psi(x, k) \, dx$$

$\mathbf{t}(k)$  is a nonlinear Fourier transform of  $q$ .

$$q = \frac{\Delta \gamma^{1/2}}{\gamma^{1/2}}$$

$$(-\Delta + q)\psi(\cdot, k) = 0$$

$$\psi(x, k) \sim e^{ikx} = e^{i(k_1+ik_2)(x_1+ix_2)}$$

### Step 1: from DN map to scattering transform

Solve traces of  $\psi$  from the boundary integral equation

$$\psi(\cdot, k)|_{\partial\Omega} = e^{ikx} - S_k(\Lambda_\gamma - \Lambda_1)\psi(\cdot, k),$$

where the single-layer operator has Faddeev Green's function as kernel.

Compute the scattering transform as

$$\mathbf{t}(k) = \int_{\partial\Omega} e^{i\bar{k}\bar{x}}(\Lambda_\gamma - \Lambda_1)\psi(x, k)d\sigma(x).$$

### Step 2: from scattering transform to $\gamma$

Define  $\mu(x, k) = e^{-ikx}\psi(x, k)$

Then the following d-bar equation holds:

$$\frac{\partial}{\partial \bar{k}} \mu(x, k) = \frac{\mathbf{t}(k)}{4\pi \bar{k}} e^{-i(kx + \bar{k}\bar{x})} \overline{\mu(x, k)}.$$

The d-bar equation has a unique solution for all  $x$ .  
The conductivity can be recovered from

$$\gamma^{1/2}(x) = \lim_{k \rightarrow 0} \mu(x, k).$$

### Practical step 1, part A: We define an approximate scattering transform

With noisy data, we cannot solve equation

$$\psi(\cdot, k)|_{\partial\Omega} = e^{ikx} - S_k(\Lambda_\gamma - \Lambda_1)\psi(\cdot, k),$$

so we introduce the approximate scattering transform:

$$\mathbf{t}^{\text{exp}}(k) = \int_{\partial\Omega} e^{i\bar{k}\bar{x}}(\Lambda_\gamma - \Lambda_1)e^{ikx}d\sigma(x)$$

We expand the exponential function as Taylor series:

$$e^{ikz} = \sum_{n=-\infty}^{\infty} a_n(k)e^{in\theta}, \quad a_n(k) = \begin{cases} \frac{(ik)^n}{n!}, & n \geq 0, \\ 0, & n < 0. \end{cases}$$

We get

$$\mathbf{t}^{\text{exp}}(k) \approx \sum_{m=0}^N \sum_{n=0}^N a_m(\bar{k})a_n(k) \langle e^{im\theta}, (\Lambda_\gamma - \Lambda_1)e^{in\theta} \rangle$$

### Practical step 1, part B: Write the approximate scattering transform in terms of data

$$\mathbf{t}^{\text{exp}}(k) \approx \sum_{m=0}^N \sum_{n=0}^N a_m(\bar{k})a_n(k) \langle e^{im\theta}, R_\gamma^{-1}e^{in\theta} \rangle - 2\pi \sum_{n=1}^N n |a_n(k)|^2,$$

where  $a_n(k) = \begin{cases} \frac{(ik)^n}{n!}, & n \geq 0, \\ 0, & n < 0. \end{cases}$

Further, we regularize the computation by truncation:

$$\mathbf{t}_R^{\text{exp}}(k) := \begin{cases} \mathbf{t}^{\text{exp}}(k), & |k| < R, \\ 0, & |k| \geq R. \end{cases}$$

### Practical step 2: solve numerically the d-bar equation with approximate kernel

Write the approximate dbar equation

$$\frac{\partial}{\partial \bar{k}} \mu_R(x, k) = \frac{\mathbf{t}_R^{\text{exp}}(k)}{4\pi \bar{k}} e^{-i(kx + \bar{k}\bar{x})} \overline{\mu_R(x, k)}$$

in integral form by applying Green's function:

$$\mu_R(x, k) = 1 + \frac{1}{\pi k} * \left( \frac{\mathbf{t}_R^{\text{exp}}(k)}{4\pi \bar{k}} e^{-i(kx + \bar{k}\bar{x})} \overline{\mu_R(x, k)} \right)$$

This Lippmann-Schwinger -type equation can be solved numerically with modified Vainikko's algorithm. Then

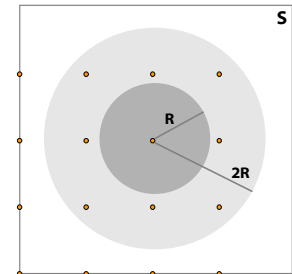
$$\gamma_R^{1/2}(x) = \mu_R(x, 0).$$

### We define a grid for numerical solution of the dbar equation with Vainikko's algorithm

The grid has  $(2^m \times 2^m)$  points in the square  $S$  in the  $k$ -plane.

Here  $m=2$ , in practice typically  $m=8$ .

This grid is suitable for the use of Fast Fourier Transform (FFT).



### The d-bar equation can be solved in a bounded domain using periodization

Instead of the d-bar equation

$$\mu_R(x, k) = 1 + \frac{1}{\pi k} * \left( \frac{t_R^{\text{exp}}(k)}{4\pi \bar{k}} e^{-i(kx + \bar{k}\bar{x})} \overline{\mu_R(x, k)} \right)$$

valid in the k-plane, we solve the S-periodic equation

$$\left[ I + \frac{1}{\pi k} * (T_R \cdot \bar{\cdot}) \right] w = 1$$

$$T_R(k) = -\frac{t_R^{\text{exp}}(k)}{4\pi \bar{k}} e^{-i(kx + \bar{k}\bar{x})}$$

The d-bar equation is also solved since it can be shown that

$$\mu_R(x, \cdot)|_{B(0, R)} = w|_{B(0, R)}$$

### Vainikko's method is based on iterative solution of linear equations

We can solve the discretized equation

$$\left[ I + \frac{1}{\pi k} * (T_R \cdot \bar{\cdot}) \right] w = 1$$

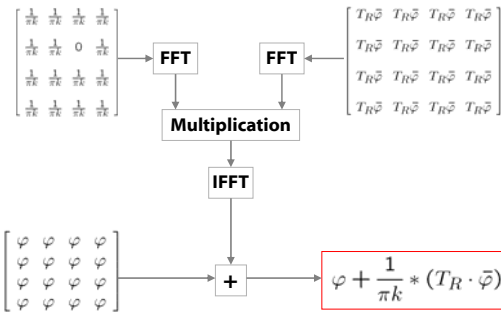
using the iterative GMRES method.

We just need to implement the formula

$$\varphi + \frac{1}{\pi k} * (T_R \cdot \bar{\varphi})$$

for a function  $\phi$  given on the grid points.

### The convolution is effectively implemented using Fast Fourier Transform (FFT)



### We have a theorem on the convergence of reconstructions when R grows

$$t_R(k) := \begin{cases} t(k), & |k| < R, \\ 0, & |k| \geq R. \end{cases}$$

$$\tilde{\mu}_R(x, k) = 1 + \frac{1}{\pi k} * \left( \frac{t_R(k)}{4\pi \bar{k}} e^{-i(kx + \bar{k}\bar{x})} \overline{\tilde{\mu}_R(x, k)} \right)$$

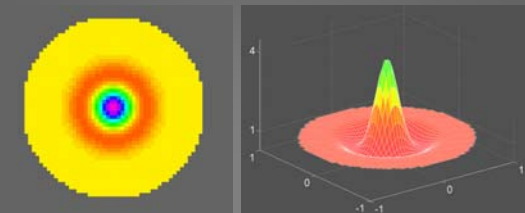
Theorem [Mueller-S 2003]: Let  $\Omega$  be the unit disc and let  $\gamma$  be  $2+m$  times continuously differentiable with  $m > 1$ .

Assume that  $\gamma=1$  near the boundary and  $0 < c < \gamma(x)$ .

Then the following estimate holds for large R:

$$\|\sqrt{\gamma} - \tilde{\mu}_R(\cdot, 0)\|_{L^\infty(\Omega)} \leq CR^{-m+1}.$$

### We construct a symmetric example conductivity

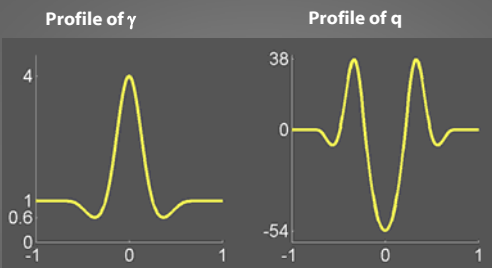


Minimum and maximum values of  $\gamma$  are 0.6 and 4

Near the boundary  $\gamma$  equals 1

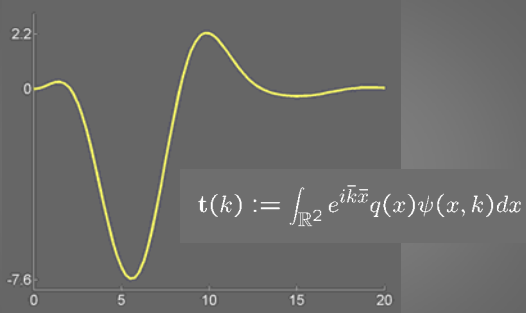
Here  $\gamma$  is 4 times continuously differentiable

### The potential q associated to $\gamma$



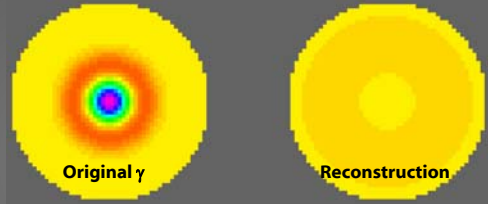
$$q = \frac{\Delta \gamma^{1/2}}{\gamma^{1/2}}.$$

We compute the scattering transform of  $\gamma$  numerically from the definition

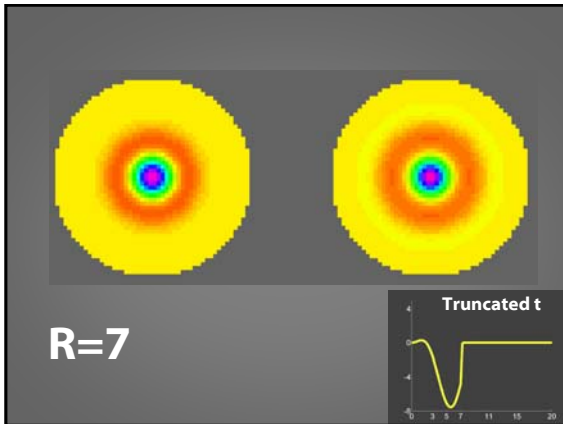
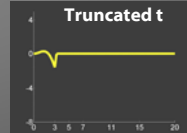


Profile of  $t$  (radial symmetry of  $q$  implies that of  $t$ )

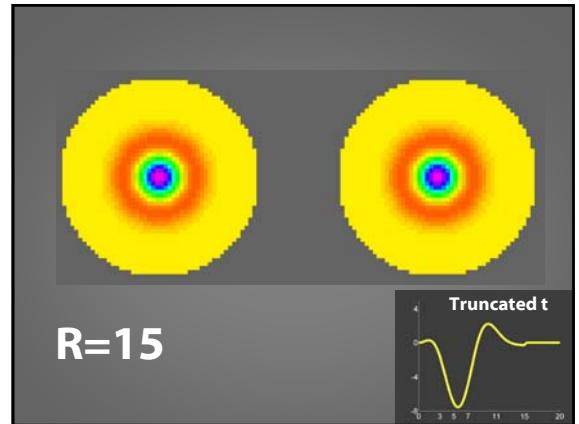
We compute the reconstruction with scattering transform truncated at  $|\mathbf{k}|=R$



$R=3$

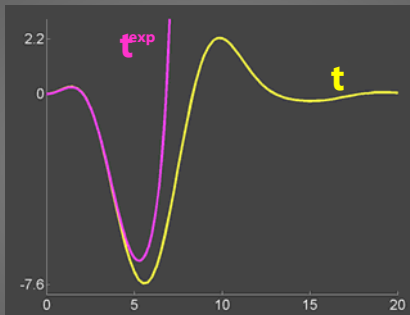


$R=7$

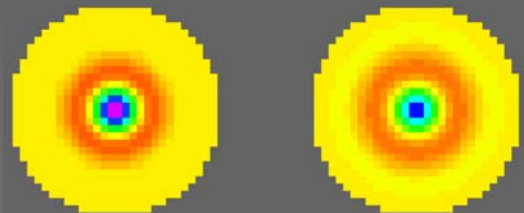


$R=15$

We compute the approximate scattering transform from noisy data



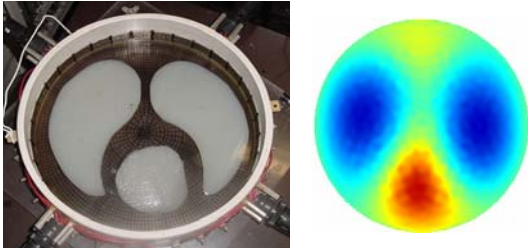
Reconstruction from noisy data



Original

Reconstruction

### Reconstruction from data measured from a chest phantom consisting of saline and agar



Relative error 23% (lung) and 12% (heart).  
Dynamical range of the reconstruction is 94% of the true range.

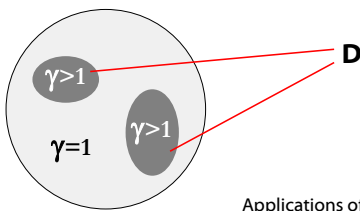
### Summary of the d-bar method

Captures correctly the order of magnitude of the difference between smallest and largest conductivity

Overall shape of the target is correct

Cannot recover discontinuities

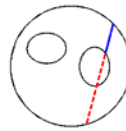
### We consider a special problem: recover the inclusion D in homogeneous background



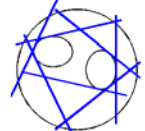
Applications of this problem:  
Nondestructive material testing  
Monitoring flow in pipelines  
Geophysical sensing

### Several approaches have been suggested to the problem of recovering inclusions

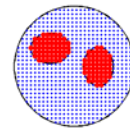
Probe method by Ikehata



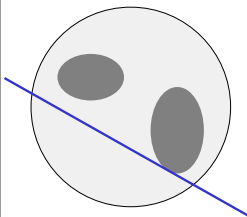
Enclosure method by Ikehata, Ohe and Siltanen



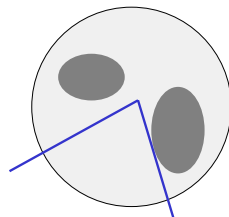
Kirsch's method by Brühl and Hanke



### The present approach is a generalization of the enclosure method



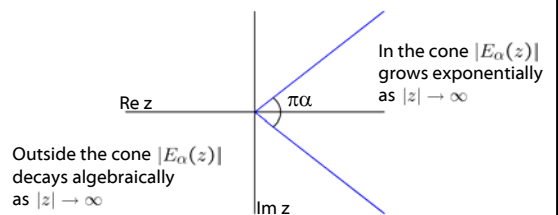
Enclosure method



Present method

### Mittag-Leffler's function: definition and asymptotic behavior

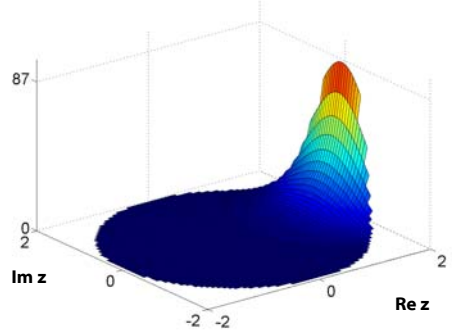
$$E_\alpha(z) = \sum_{m=0}^{\infty} \frac{z^m}{\Gamma(\alpha m + 1)}$$



**Mittag-Leffler's function**  
has a closed form expression for  $\alpha=1/2$

$$E_{1/2}(z) = e^{z^2} \left\{ 1 + \frac{2}{\sqrt{\pi}} \int_0^z e^{-u^2} du \right\}$$

This is a plot of the absolute value  
of Mittag-Leffler's function ( $\alpha=1/2$  and  $|z|<2$ )



**Indicator function is the key object**  
for recovering the inclusion from the DN map

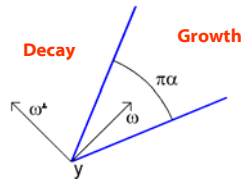
Set

$$I_{(y,\omega)}^\alpha(\tau) = \int_{\partial\Omega} \frac{\partial e_\tau^\alpha}{\partial \nu} (R_1 - R_\gamma) \frac{\partial e_\tau^\alpha}{\partial \nu} d\sigma,$$

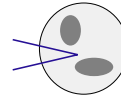
where

$$e_\tau^\alpha(x; y, \omega) = E_\alpha(\tau\{(x-y)\cdot\omega + i(x-y)\cdot\omega^\perp\}).$$

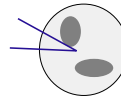
Asymptotic behavior  
of  $e_\tau^\alpha$  as  $|z| \rightarrow \infty$ :



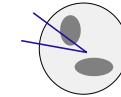
**Theorem 1: for a given cone C, we can**  
**find out if C intersects the inclusion D**



$$\lim_{\tau \rightarrow \infty} |I_{(y,\omega)}^\alpha(\tau)| = 0$$

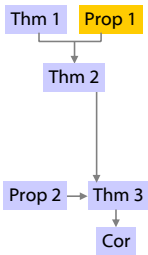


$$\liminf_{\tau \rightarrow \infty} |I_{(y,\omega)}^\alpha(\tau)| > 0$$



$$\lim_{\tau \rightarrow \infty} |I_{(y,\omega)}^\alpha(\tau)| = \infty$$

**Proposition 1 shows that truncated indicator**  
**function converges to the indicator function**



**Definition.** For  $N \geq 1$ , truncated indicator function is

$$I_{(y,\omega)}^{1/n,N}(\tau) = \int_{\partial\Omega} (\Lambda_\gamma - \Lambda_1) g \cdot \bar{g} d\sigma,$$

$$g(x) = E_{1/n}^N(\tau\{(x-y)\cdot(\omega + i\omega^\perp)\}),$$

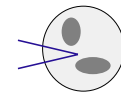
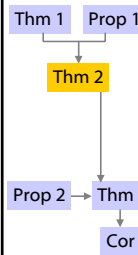
where  $E_{1/n}^N(z)$  is truncated power series.

**Proposition 1.** Let  $n \geq 2$  and  $N \geq 1$ . Then

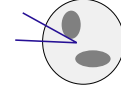
$$\lim_{N \rightarrow \infty} |I_{(y,\omega)}^{1/n}(\tau_N) - I_{(y,\omega)}^{1/n,N}(\tau_N)| = 0.$$

The convergence is uniform with respect to  $\omega$ .

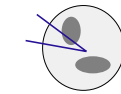
**Theorem 2 shows that the conclusion of Thm 1**  
**holds for truncated indicator function**



$$\lim_{N \rightarrow \infty} |I_{(y,\omega)}^{1/n,N}(\tau_N)| = 0;$$



$$\liminf_{N \rightarrow \infty} |I_{(y,\omega)}^{1/n,N}(\tau_N)| > 0;$$



$$\lim_{N \rightarrow \infty} |I_{(y,\omega)}^{1/n,N}(\tau_N)| = \infty.$$

**Proposition 2: when noise level tends to zero, error in indicator function vanishes**

Thm 1 Prop 1

Thm 2

Prop 2 → Thm 3

Cor

**Definition.** Let  $(y, \omega) \in \Omega \times S^1$ . Define the noisy truncated indicator function by the formula

$$I_{(y, \omega)}^{1/n, nN}(\tau; \mathcal{E}^{nN}) = \sum_{0 \leq m, \ell \leq nN} \frac{\tau^{m+\ell}}{\Gamma(\frac{m}{n} + 1)\Gamma(\frac{\ell}{n} + 1)}$$

$$\times \int_{\partial\Omega} \{(\Lambda_\gamma - \Lambda_1) \cdot ((x - y) \cdot (\omega + i\omega^\perp))\}^m \cdot \mathcal{E}_m^1(x) \cdot \{(\omega + i\omega^\perp) \cdot (x - y)\}^\ell + \mathcal{E}_\ell^1(x) \} d\sigma(x).$$

**Proposition 2.** Let  $n \geq 2$ . For  $N = N(\delta; y)$  we have

$$\sup_{\|\mathcal{E}^{nN}\| \leq \delta} |I_{(y, \omega)}^{1/n, nN}(\tau_N; \mathcal{E}^{nN}) - I_{(y, \omega)}^{1/n, nN}(\tau_N)| = O(\delta^{1-\theta}) \log \delta^{(2n-1)/n}$$

as  $\delta \rightarrow 0$ . The convergence is uniform with respect to  $\omega$ .

**Theorem 3: when noise level tends to zero, reconstruction from noisy data is possible**

Thm 1 Prop 1

Thm 2

Prop 2 → Thm 3

Cor

$\limsup_{\delta \rightarrow 0} \sup_{\|\mathcal{E}^{nN}\| \leq \delta} |I_{(y, \omega)}^{1/n, nN}(\tau_N; \mathcal{E}^{nN})| = 0;$

$\liminf_{\delta \rightarrow 0} \inf_{\|\mathcal{E}^{nN}\| \leq \delta} |I_{(y, \omega)}^{1/n, nN}(\tau_N; \mathcal{E}^{nN})| > 0;$

$\liminf_{\delta \rightarrow 0} \inf_{\|\mathcal{E}^{nN}\| \leq \delta} |I_{(y, \omega)}^{1/n, nN}(\tau_N; \mathcal{E}^{nN})| = \infty.$

**Corollary: when noise level tends to zero, reconstruction from finite noisy data possible**

Thm 1 Prop 1

Thm 2

Prop 2 → Thm 3

Cor

$\limsup_{\epsilon \rightarrow 0} \sup_{\|\mathcal{E}^{nN}\| \leq \epsilon} |I_{(y, \omega)}^{1/n, nN}(\tau_N; \mathcal{E}^{nN})| = 0;$

$\liminf_{\epsilon \rightarrow 0} \inf_{\|\mathcal{E}^{nN}\| \leq \epsilon} |I_{(y, \omega)}^{1/n, nN}(\tau_N; \mathcal{E}^{nN})| > 0;$

$\liminf_{\epsilon \rightarrow 0} \inf_{\|\mathcal{E}^{nN}\| \leq \epsilon} |I_{(y, \omega)}^{1/n, nN}(\tau_N; \mathcal{E}^{nN})| = \infty.$

**Indicator function can be written in terms of the measured ND map**

Write  $I_{(y, \omega)}^\alpha(\tau) = \int_{\partial\Omega} \frac{\partial e_\tau^\alpha}{\partial \nu} (R_1 - R_\gamma) \frac{\partial e_\tau^\alpha}{\partial \nu} d\sigma,$

and expand the function  $\frac{\partial e_\tau^\alpha}{\partial \nu}$  in Fourier basis to get

$$I_{(y, \omega)}^{1/n, nN}(\tau) = 2\pi \sum_{1 \leq m, \ell \leq nN} \frac{\tau^{m+\ell} \omega^m \omega^\ell}{\Gamma(\frac{m}{n} + 1)\Gamma(\frac{\ell}{n} + 1)}$$

$$\times \sum_{r_1=1}^m \sum_{r_2=1}^\ell \binom{m}{r_1} \binom{\ell}{r_2} r_1 r_2 (-1)^{m+\ell-r_1-r_2} y^{m-r_1} \bar{y}^{\ell-r_2}$$

$$\times (\mathcal{R}_1[r_2, r_1] - \mathcal{R}_\gamma[r_2, r_1]).$$

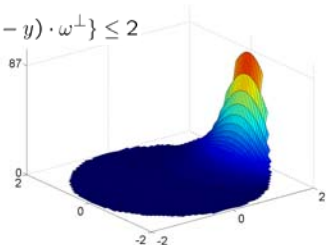
**Due to the finite number of measurements, we cannot take  $\tau$  to infinity**

The truncated power series of Mittag-Leffler's function gives relative accuracy of 1% for  $|z| < 2$ . We evaluate Mittag-Leffler's function at

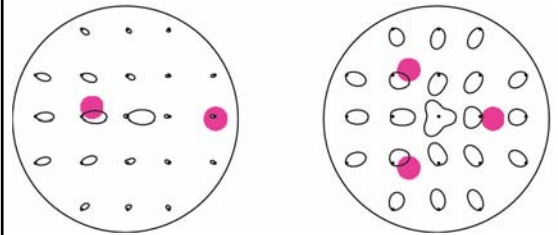
$$\tau \{(x - y) \cdot \omega + i(x - y) \cdot \omega^\perp\} \leq 2$$

Thus we choose

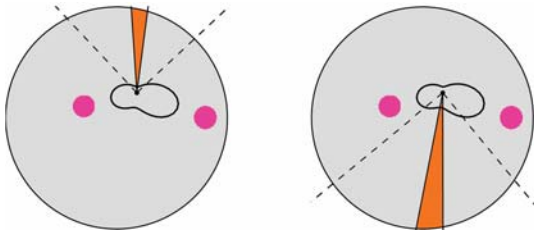
$$\tau(y) = \frac{1}{1 + |y|}$$



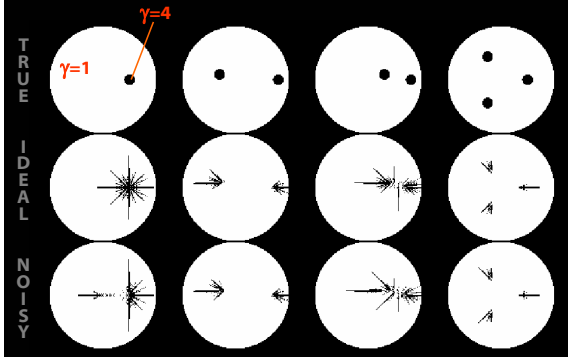
**Examples of indicator functions**



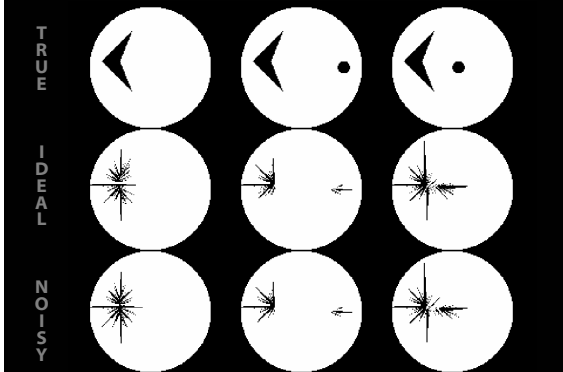
**Our reconstruction strategy is to exclude cones giving local minima of the indicator function**



**Numerical example of recovering disc inclusions**



**Recovering nonconvex inclusions**



**Summary of the inclusion detection method**

- Finds the number and location of inclusions
- No regularization parameter needed
- Shape of inclusions not recovered

**In the future we face the following challenges:**

- Modelling electrode measurements properly
- Analysing the approximation and truncation of  $t(k)$
- Recovering inclusions in nonconstant but known background
- Developing 3-D algorithms
- Inverse obstacle scattering with Mittag-Leffler's function

**References**

- 2000 **Siltanen S, Mueller J L and Isaacson D**, *An implementation of the reconstruction algorithm of A. Nachman for the 2-D inverse conductivity problem*, *Inverse Problems* 16, 681-699
- 2000 **Ikehata M and Siltanen S**, *Numerical method for finding the convex hull of an inclusion in conductivity from boundary measurements*, *Inverse Problems* 16, 1043-1052
- 2003 **Mueller J L and Siltanen S**, *Direct reconstructions of conductivities from boundary measurements*, *SIAM J. Scientific Computation* 24(4), 1232-1266
- 2004 **Knudsen K, Mueller J L and Siltanen S**, *Numerical solution method for the dbar-equation in the plane*, to appear in *J. Comp. Phys.*